Detection of Step Changes in Real-World Synchrophasor Measurements

Mohammad MansourLakouraj[1], *Student Member, IEEE*, Chetan Mishra[2], *Member, IEEE*, Jaime De La Ree Jr.[2], Luigi Vanfretti[3], *Senior Member, IEEE*, Kevin D. Jones[2], and Hanif Livani[1], *Senior Member, IEEE*
[1]Department of Electrical & Biomedical Engineering, University of Nevada, Reno, Reno, NV
[2] Dominion Energy, Richmond, VA
[3] ECSE Department, Rensselaer Polytechnic Institute, Troy, NY

2024 IEEE Power & Energy Society General Meeting (PESGM) | 979-8-3503-8183-2/24/$31.00 ©2024 IEEE | DOI: 10.1109/PESGM51994.2024.10688944

***Abstract*—This paper presents a practical method for detecting step changes in real-world synchrophasor measurements based on three fundamental theories. Step changes can be caused by shunt switching, generator set point changes, and other changes in grid apparatus, and detecting them is important for understanding the grid's response to inverter-based resources. To precisely localize step changes, a *nonorthogonal* discrete wavelet transformation (DWT) based on smoothed gradient estimation is used. A detector based on a multiscale *point-wise product* of wavelet coefficients is proposed, which takes advantage of the broadband characteristic of step changes in the wavelet coefficient space. This product also suppresses undesirable signal components, thereby reducing false positives. Finally, Rosin's *unimodal thresholding* is used to provide an adaptive threshold for the step detector. The effectiveness of the proposed approach is demonstrated on synthetic signals and real-world synchrophasor data obtained from Dominion Energy's power grid.**

***Index Terms*—step detection, synchrophasors, nonorthogonal wavelets, multiscale products, Rosin thresholding.**

I. Introduction

Phasor measurement units (PMUs) provide high-precision, synchronized time series data from multiple locations, allowing utilities to perform advanced, real-time, wide area monitoring [1] of different dynamics of the power system. A monitoring tool that exploits PMU data to continuously monitor electromechanical oscillations arising from degraded grid conditions, known as a "mode meter", provides alerts to operators to take remedial actions when the damping of specific modes decreases [1]. Such monitoring tools can also enable the use of new control schemes, thus mitigating the impact of such oscillations [1]. Another dynamic pheonomena at a slower time scale that may arise due to weakened power grid conditions is voltage instability. To address this, data-driven techniques use an approximate model (Thevenin equivalent [2]) of the grid to detect the emergence of voltage instability.

A major obstacle in solving these monitoring problems in practice is that there are numerous components that interact with the grid simultaneously, so it is essential to select the suitable data window, where the relevant dynamics of the grid are predominant. When concerned in monitoring deteriorating grid conditions, this can be addressed by finding instances with step changes in relevant variables (e.g. voltage magnitude, active/reactive power of a power plant, etc.), which is the focus of this paper.

Several PMU applications exploit signal processing techniques as an effective means to extract and analyze the relevant dynamics of the power system present in the measurement data. These have proven to be effective in assessing dynamic performance driven by data from normal operation (ambient conditions) [1], [2]. Other applications of interest for the work in this paper include event detection and classification algorithms [3] that extract unique signal attributes in the time domain. Meanwhile, in [4], an orthogonal wavelet transformation is used for event detection in real-world applications. Constructing an "event" detector typically requires selecting an appropriate set of basis functions, i.e. the mother wavelet, to act as filters that extract a significant component from the signal. After that, it is necessary to determine an appropriate threshold for the 'filtered signal,' which is a difficult task in itself and is only vaguely discussed in previous research, relying on prior knowledge about ambient data, and thus is addressed herein.

Step and edge detection algorithms have conventionally relied on smoothed gradient estimation of signals. Within this context, the Gaussian derivative has gained popularity as a technique among filtered derivative methods [5]. Since the selected scale has a considerable impact on detection performance, derivative estimation with simultaneous multiscale smoothing was proposed in [6]. On the other hand, it is recognized that wavelets are needed to detect local signal regularity and singularity on different scales [7]. Therefore, bridging the gap between wavelet transformation and the smoothed gradient estimation in multi-level smoothing could be a potential solution for enhanced step/edge detection. To this end, an efficient *non-orthogonal* discrete wavelet transformation (DWT) was proposed in [8] that uses a smooth gradient estimation and adjusts the smoothing level depending on the (dyadic) scale. In order to achieve this, quadratic spline wavelets that imitate the derivative of the Gaussian estimator are employed to maintain regularity information for each point at each scale in time and identify the singularities. This technique is also called Mallat and Zhong (MZ)-DWT. It is important to emphasize that MZ-DWT is capable of recognizing various points of abrupt changes in the signal, including step-like shapes. In this paper, we extend this approach by analyzing multiscale

This material is based upon work supported by the U.S. National Science Foundation under Grant ECCS-2033927.

wavelet transformations. The MZ-DWT is able to maintain a strong relationship between different scales while still keeping the same time frame for all scales. Thus, multiscale pointwise noise products [9] can be used to amplify multiscale peaks associated with steps in the measurement data while simultaneously damping and other sharp variations [6].

The application of the multiscale product theory reduces noise, leading to a data set with few step-related features, such as sharp peaks, and many values close to zero. Consequently, the distribution function of this data set is unimodal, primarily centered around zero, with a negligible peak at the end of the tail. This feature allows us to utilize Rosin's unimodal thresholding technique [10], which effectively differentiates the group of zeros (noise signatures) from the step-related signatures, thus greatly improving the automated detection process. In the following section, the proposed methodology is given in Section II. The Numerical Analysis is presented in Section III. Finally, we conclude the paper in Section IV.

II. Proposed Step Detection Approach

A. Nonorthogonal Discrete Wavelet Transform

The step/edge detection methods work by first smoothing the signal at different scales and then detecting points of abrupt changes by examining the derivatives of the signal. Within this context, the derivative of Gaussian has become an effective method among the edge detection approaches, calculating the gradient after applying a Gaussian smoothing function in different scales [5]. The authors of [8] introduce a discrete wavelet transformation equipped with smoothed derivative estimation and Gaussian to detect edges, which we briefly present as follows.

The smoothing function $\phi(t)$, such as Gaussian, is defined as a function for which the integral equals 1 and as t tends to infinity, the function converges to zero. The derivative of the Gaussian function is denoted as $\theta(t) = \frac{d\phi(t)}{dt}$. The derivative of this smoothing function shares the property of wavelets, as its integral equals zero, represented as $\int_{-\infty}^{+\infty} \theta(t)\, dt = 0$. Subsequently, the wavelet transforms are computed by convolving the signal $g(t)$ with a re-scaled wavelet, given as

$$W_s g(t) = g(t) * \theta_s(t) \tag{1}$$

where $\theta_s(t) = \frac{\theta(t/s)}{s}$, introducing a re-scaled derivative of Gaussian function at the scale s. Now, the wavelet transform is modified as

$$W_s g(t) = g(t) * (s\frac{d\phi_s}{dt})(t) = s\frac{d}{dt}(g(t) * \phi_s)(t). \tag{2}$$

The equation (2) operates as a derivative estimation of the smoothed signal at the scale s, meaning that the local extrema of this transformation are corresponding with the inflection points of $g(t) * \phi_s$. The degree of smoothing depends on the adjusted scales. However, selecting scales varying on dyadic sequence $\left(2^j\right)_{j\in\mathbb{Z}}$ is the superior choice when compared to continuous scale s, minimizing the computational burden. The discrete filters N and M define the characteristics of the quadratic wavelet. The subsequent algorithm is used to compute the Discrete Wavelet Transform (DWT) for the discrete synchrophasor measurements [8].

Algorithm 1: MZ-DWT

Data: Synchrophasor measurements, discrete filters of quadratic splines (N, M), number of scales (J).
Result: Discrete wavelet transforms in different scales
Initialization; $j = 0$
while $j < J$ **do**
- $\mathrm{W}^d_{2^{j+1}}\, g = \frac{1}{\lambda_j}\, \mathrm{S}^d_{2^j}\, g * M_j$;
- $\mathrm{S}^d_{2^{j+1}}\, g = \mathrm{S}^d_{2^j}\, g * N_j$;
- $j = j + 1$

end

In Algorithm 1, λ_j denotes the *normalization coefficient* for the quadratic wavelet. The *finite responses* of the filters N and M associated with the quadratic wavelet are provided in the Appendix of [8].

B. Multiscale Products

Researchers have examined how the noise and singularity in the signal behave at different wavelet scales using the *Lipschitz regularity* concept [11]. Singularities have a greater degree of Lipschitz regularity, meaning that they follow a more consistent behavior compared to noises. For instance, the step change on the measurements has a Lipschitz regularity of zero, while structures less smooth than a step possess negative regularity. On the other hand, white noise appears almost singular, maintaining a uniform regularity that equates to -0.5.

A theory is introduced that relates the evolution of wavelet transformation magnitude with Lipschitz regularity of the signal [12]. A signal denoted as $g(t)$ is considered uniformly Lipschitz c $(0 < c < 1)$ within the range $[t_1, t_2]$ if and only if there exists a positive constant N for all values in the range, the wavelet transformation is constrained as $|W_{2^j} g(t)| \leq N(2^j)^c$.

This constraint indicates that as the scale increases, the wavelet transforms' magnitude increases when c is positive. Conversely, the magnitudes of the wavelet transform get smaller as the scale increases for the negative value of c. By adopting MZ-DWT, The signal's singularities change over different scales, with noticeable peaks, while noise diminishes significantly across the scales. Thus, we can visualize that when the DWT is multiplied at consecutive scales, it magnifies the characteristics of edges while diminishing the impact of noise. Thus, the multiscale product of B scales is defined as

$$m_B(t) = \prod_{i=1}^{B} W_s g(t). \tag{3}$$

C. Unimodal Thresholding

Rosin's method is developed for thresholding unimodal distribution of multiscale products and is recognized as a remarkably straightforward approach [10]. This method assumes that there is a dominant group within the data, resulting in a prominent peak positioned toward the lower section of the histogram relative to the second population. The second population associated with the step-related feature *may not*

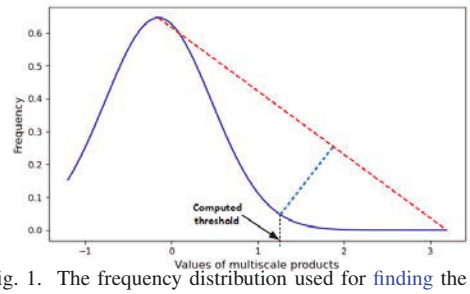

Fig. 1. The frequency distribution used for finding the threshold

exhibit distinguishable peaks but should indicate a reasonable degree of separation from the main peak.

A typical distribution function, which usually has one obvious peak, is shown in Fig. 1. To define the thresholding, we need to fit a realistic distribution function to the histogram of our data, allowing us to work with the data points on this function. To find the function, we employ the kernel density estimate (KDE) approach. Next, the straight line is sketched from the highest point of the distribution function to the end of the final populated bin in its histogram. The threshold point is optimized in such a way that the perpendicular distance (shown with a blue dotted line) between the red line and the optimal point on the distribution function is *maximized*. Then, the black dotted line gives the value of the threshold at the optimal point of the intersection with the x-axis. These steps are performed with Rosin's algorithm.

III. Numerical Assessment

In this section, the competence of the proposed framework is shown by performing an analysis of synthetic data and field PMU data on the service territory of the utility. Synchrophasor data with a reporting rate of 30 phasors per second are available through the digital fault recorders in the substations. We select positive sequence voltage magnitude data to examine our approach. We also employ two effective thresholding methods for comparison [13]: 1) the mean plus three times the standard deviation, referred to as SD, and 2) the median plus three times the median absolute deviation, named MAD.

A. Case 1

A synthetic signal, encompassing steps, large spikes, ramping, and noise, is simulated for the purpose of conducting a step detection test. Step changes result from set point adjustments, capacitor bank and breaker switching, and controller responses. Transient disturbances commonly induce spikes, while ramping is primarily caused by generation unit output adjustments and voltage regulator actions. Algorithm 1 is used to obtain the wavelet transformations. The dyadic wavelet transformations of the signal, as shown in Fig. 2(a), are obtained and illustrated in Figs. 2(b) to 2(e). This transformation, enabled by the Gaussian derivative (quadratic spline), indicates the derivative estimation of the original signal at different levels of smoothing. Our proposed method preserves the length of the transformation as the original signal, keeping the regularity information at each sample (time) on every scale.

The first scale, shown in Fig. 2 (b), includes high-frequency variations, including the large spikes on the signal located at sample 75 and 140. The features corresponding to large spikes in the original signal are represented as two consecutive spikes in opposite directions. Specifically, when a spike in the signal points downward, the wavelet transformation represents it with an initial spike in the negative direction. Conversely, when the spike points upward in the measurement, its transformation is depicted on the positive side of the y-axis. This distinctive feature associated with the spikes of the signal can also be seen on the second scale, but it becomes less pronounced from the third scale. Similarly, noises are being filtered more efficiently on the larger scales. Consequently, the increased smoothing on larger scales leads to a reduction in the magnitude of local extrema seen due to noise.

In addition, the signal includes four small step changes happening in samples 30, 60, 100 and 150. The effect of these steps can be seen better on larger scales because the convolution of the signal with derivative of the smoother function eliminates small and narrow fluctuations in the signal. More specifically, the step occurring in sample 30 moves upward, and all transformations in four scales show this step with local maxima. The other three steps are also characterized with local extrema in the downward direction across all scales of wavelet transforms. The MZ-DWT helps in preserving edge-like features and closely finding instance of occurrence.

The multiscale relationships are clearly observable in the presence of step changes. To enhance the multi-scale peaks associated with the steps and then establish a robust threshold, the multi-scale pointwise product is implemented. Fig. 3 shows the result of this product for scales 3 and 4. All scales together or other scales can be chosen, but in smaller scales, we see more false local extrema, even though the steps are localized more accurately. In addition, fewer local extrema can be seen when a larger scale is selected, but the accuracy in locating the time of occurrence of the steps may slightly reduced. In this case (and in the following cases), the product of two adjacent scales (3 and 4) is considered, preserving both the advantages of detection and localization by suppressing noise and sharpening step-type features [7]. Now, the product of scales is statistically characterized to establish a robust threshold to differentiate step-related changes from other variations. This happens because when we have large spikes or severe noises on the signal, their impact can still be seen on the product of the scales, although they are becoming smaller shapes in this transformation. Thus, one may interpret them as step changes in the multiscale product series, as they are essentially smaller maxima. This fact necessitates the use of a threshold to distinguish steps from other transient and sharp variations. Since the product of scales comprises many values close to zero and only a few values larger than that (associated with edges), its histogram follows a unimodal pattern centered around zero. That is why Rosin's unimodal thresholding is selected. First, we fit a function to the histogram using KDE. As shown in Fig. 3, the unimodal threshold can effectively catch four peaks associated with small steps, while separating

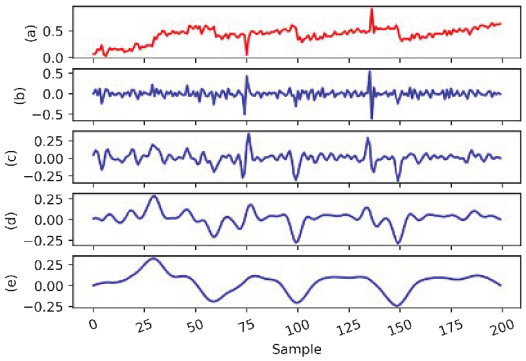

Fig. 2. An illustration of MZ-DWT, showing (a) the comprehensive signal, and (b) to (e) the initial four scales of the DWT.

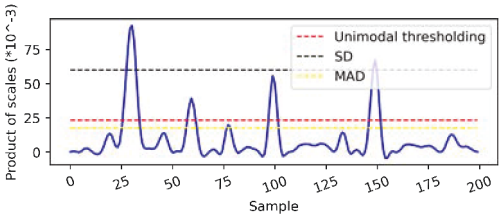

Fig. 3. The product of scales and the computed threshold for Case 1

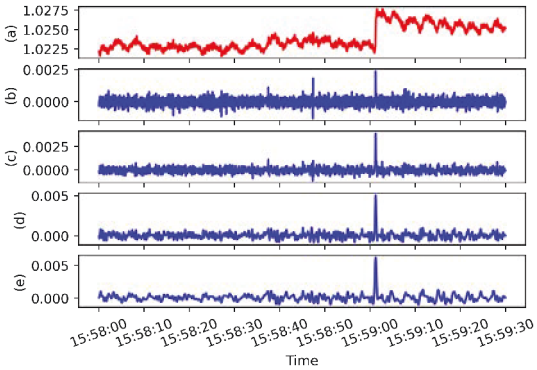

Fig. 4. An illustration of MZ-DWT, showing (a) the voltage time series, and (b) to (e) the initial four scales of the DWT.

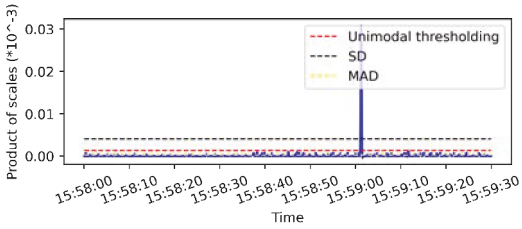

Fig. 5. The product of scales and the computed threshold for Case 2

smaller peaks associated with large spikes and noise below the dotted red threshold line. However, Fig. 3 demonstrates that the SD threshold only detects two steps, while the MAD threshold exhibits conservative performance by detecting all steps and one large spike, resulting in a false alarm.

B. Case 2

In this scenario, the voltage time series is recorded by a PMU situated on the substation of the 115 kV solar power plant. The reporting rate of the PMU is 30 values per second, and we have chosen a 90-second window for analysis. As shown in Fig. 4(a), the voltage indicates some oscillations that appear in this region near the solar power plant. A step change with a small magnitude of 0.005 p.u. (0.33 kv) occurs around 15:59:02. Wavelet transformations are shown on different scales in Figs. 2(b) to 4(e). All transformations indicate large spikes moving upwards when the step rises. Furthermore, the multiscale products are indicated in Fig. 5, damping the noise and variations with higher frequencies associated with oscillations. The time of the step change is also closely maintained in the product of scales. The robustness of the threshold is again indicated in Fig. 5, since it could differentiate undesired variations from sudden step-related changes in the multiscale product time series. Furthermore, SD detects the step accurately, while MAD shows conservative performance by detecting all steps and several spikes associated with oscillations and noise, resulting in several false alarms.

C. Case 3

In this section, we illustrate the line voltage recorded by a PMU located in a real-world substation. The PMU provides phasor estimates, which are reported at a rate of 30 estimates per second. We have "downsampled" these estimates from the stream of PMU data, which can be regarded as samples of a function reporting at 1 sample per second to evaluate our approach under slower dynamics. Please note that the values obtained from the PMU represent the outcomes of multiple measurements and are not samples of a signal. The field voltage measurements are shown in Fig. 6(a) for two hours. This signal consists of two small steps and two relatively large steps. The first step change, which resulted in the largest measurement change, is due to the CB switching in the local under-study substation. This is why the voltage increases more than other step changes caused by other sources. The magnitude of the step can be used as an identifier to locate the source of the changes.

At each dyadic scale, a uniform length of the transformation is obtained in the wavelet domain, as shown in Figs. 6(b) to 6(e). The step changes are detected precisely on scales three and four of wavelet transforms because the smoothing with the Gaussian at higher scales vanishes noises and abrupt pulses while preserving step-related features. On the other hand, two small steps are not distinguishable at scale 1, as this scale contains higher-frequency information. However, the impact of small steps can still be detected at scale 2. Since the extrema appear due to steps in wavelet transformations and are transmitted across scales 3 and 4, the product of these extrema tends to reinforce the voltage signal response. Fig. 7 clearly indicates that the point product effectively preserves step responses and closely pinpoints the step rise time.

The Rosin thresholding effectively separates four step-related signatures from other variations. Fig. 7 shows that SD is unable to detect the smallest step's signature, while MAD exhibits conservative performance by detecting several noise-

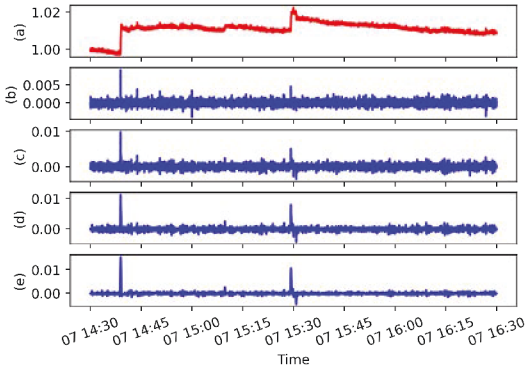

Fig. 6. An illustration of MZ-DWT, showing (a) the voltage time series, and (b) to (e) the initial four scales of the DWT.

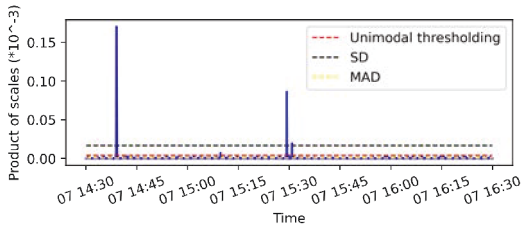

Fig. 7. The product of scales and the computed threshold for Case 3

related features. Note that there are limited options available for thresholding unimodal distributions, which is why we recommend using Rosin's method.

D. Orthogonal Daubechies Wavelet

Daubechies 1 (db1) with an orthogonal basis is selected to discuss its performance in the problem due to its promising performance in detection [4]. The db1 wavelet is sensitive to sharp changes, which is intuitive as it uses a step-like wavelet. We also examined db2-db8, which shows a poorer detection performance compared to db1, which was also proved in [4]. Fig. 8 illustrates the db1 transformation for Case 3, where the scales are not of the same length, unlike the results of the complete MZ-DWT. As a result, db1 cannot precisely localize the time of the changes. Furthermore, we cannot find a single scale that can pinpoint all four steps with different magnitudes simultaneously, whereas the proposed MZ-DWT effectively reveals these evolving step features on various scales, especially larger ones. Additionally, the proposed product theory and threshold are not applicable to db1 with orthogonal scales with varying lengths that cannot preserve edge features on different scales at the same data points. As a result, the process of these transforms and choosing an appropriate scale for detection can be a challenging task for real-world data analytics. Then, thresholding needs to be done separately on each scale for db1 and other orthogonal wavelets, which may lack sufficient information about small steps commonly found in the *ambient* data analysis, leading to poor detection performance.

IV. Conclusions

This paper proposed an effective framework for detecting step-like patterns in real-world synchrophasor data, which is a growing need for power system studies in the utility. Many changes in the system manifest as steps in the synchrophasor

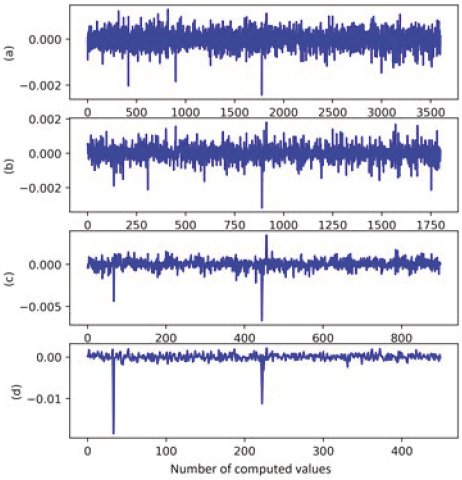

Fig. 8. The db1 transformation, showing four scales from (a) to (d).

data, and accurate detection of these steps greatly aids in identifying the type and source of changes, understanding controller responses, detecting events, and classifying them to enhance situational awareness.

The nonorthogonal wavelet transformation, based on smoothed gradient estimation, was used to identify singularities in the signals. Then, multiscale product theory was applied to effectively extract step-related features by filtering out noise. Finally, the Rosin threshold provided effective detection performance to complete the automation loop. The proposed approach was able to detect the small and large step changes in synchrophasor data effectively while providing information on the *instant* of the step changes.

References

[1] D. Kosterev et al, "Implementation and operating experience with oscillation detection applicatioin at bonneville power administration," in *CIGRE 2016 Grid of the Future Symposium*, 2016, pp. 1–12.
[2] J. Lavenius et al, "Performance assessment of pmu-based estimation methods of thevenin equivalents for real-time voltage stability monitoring," in *2015 IEEE 15th EEEIC*, 2015, pp. 1977–1982.
[3] Y. Liu et al, "Robust event classification using imperfect real-world PMU data," *IEEE Internet of Things Journal*, 2022.
[4] D.-I. Kim et al, "Wavelet-based event detection method using pmu data," *IEEE Transactions on Smart Grid*, vol. 8, no. 3, pp. 1154–1162, 2017.
[5] J. Canny, "A computational approach to edge detection," *IEEE Transactions on Pattern Analysis and Machine Intelligence*, vol. PAMI-8, no. 6, pp. 679–698, 1986.
[6] B. Sadler and A. Swami, "Analysis of multiscale products for step detection and estimation," *IEEE Transactions on Information Theory*, vol. 45, no. 3, pp. 1043–1051, 1999.
[7] P. Bao and L. Zhang, "Noise reduction for magnetic resonance images via adaptive multiscale products thresholding," *IEEE Transactions on Medical Imaging*, vol. 22, no. 9, pp. 1089–1099, 2003.
[8] S. Mallat and S. Zhong, "Characterization of signals from multiscale edges," *IEEE Transactions on Pattern Analysis and Machine Intelligence*, vol. 14, no. 7, pp. 710–732, 1992.
[9] A. Rosenfeld, "A nonlinear edge detection technique," *Proceedings of the IEEE*, vol. 58, no. 5, pp. 814–816, 1970.
[10] P. L. Rosin, "Unimodal thresholding," *Pattern recognition*, vol. 34, no. 11, pp. 2083–2096, 2001.
[11] S. Mallat and W. Hwang, "Singularity detection and processing with wavelets," *IEEE Transactions on Information Theory*, vol. 38, no. 2, pp. 617–643, 1992.
[12] Y. Meyer, "Ondelettes et opérateurs," *New York: Hermann,*, 1990.
[13] C. Leys et al, "Detecting outliers: Do not use standard deviation around the mean, use absolute deviation around the median," *Journal of experimental social psychology*, vol. 49, no. 4, pp. 764–766, 2013.